Simulation of gas production in the northern regions: the role of thermodynamics

E.A. Bondarev
Institute of Oil and Gas Problems
Siberian Branch, Russian Academy of Sciences
Yakutsk, Russia
e-mail: bondarev@ipng.ysn.ru

I.I. Rozhin
Institute of Oil and Gas Problems
Siberian Branch, Russian Academy of Sciences
Yakutsk, Russia
e-mail: bondarev@ipng.ysn.ru

K.K. Argunova
Institute of Oil and Gas Problems
Siberian Branch, Russian Academy of Sciences
Yakutsk, Russia
e-mail: bondarev@ipng.ysn.ru

Abstract[1]

The influence of mathematical model parameters on the dynamics of pressure and temperature fields at non-isothermal gas filtration is investigated in a numerical experiment. A nonlinear system of partial differential equations obtained from the energy and mass conservation laws and the Darcy law are used to describe the process, and physical and caloric equations of state are used as closing relations. The boundary conditions correspond to a given pressure drop at the bottom hole. It is shown that the influence of the temperature field on such integral characteristics as cumulative gas production is most pronounced at moderate pressure drops. The size of the zone of possible hydrate formation in a gas reservoir is determined in two particular examples.

Nomenclature

c_p – specific heat of the gas;

c_r – volume heat of the reservoir filled with the gas;

H – reservoir thickness;

h – grid step in space, $\overline{\omega}_h = \{r_i = r_w + ih,\ i = \overline{0, n}\}$

k – permeability of the reservoir;

l – characteristic size;

M – mass production of the gas;

m – porosity;

p – pressure;

R – gas constant;

r – radial coordinate;

s – iteration step;

T – temperature;

t – time;

Z– coefficient of gas imperfection;

κ_p –piezoconductivity of the reservoir saturated with the gas;

μ – dynamic viscosity of the gas;

τ – grid step in time, $\overline{\omega}_\tau = \{t_j = j\tau,\ j = \overline{0, j_0}\}$.

1. Introduction

Natural gas extraction (especially in regions of Siberia and extreme north) can involve conditions favoring the formation and deposition of hydrates in wells and bottom holes. At the moment, these processes are considered separately, i.e., the dynamics of hydrate formation in various production modes is modeled within the framework of non-isothermal multiphase filtration, while the dynamics of hydrate formation in wells is studied within the framework of tube hydraulics [1–3]. In the latter case, the temperature and pressure near the bottom hole are specified and are normally assumed to be equal to their reservoir values [1, 2]. An attempt to combine these two problems was made in a recent publication [4]. The authors [4], however, confined themselves to determining the temperature and pressure fields in the reservoir, while the dynamics of growth of the hydrate layer in the well was determined within the framework of the model proposed in [1], i.e., the problem of determining the possibility of hydrate formation in the bottom hole zone was not even posed. Moreover, the condition of a zero heat flux was imposed on the interface between the reservoir and the well in [4], whereas the heat flux on this interface differs from zero in reality and is physically determined by convective transport and cooling of the gas during its throttling. The first attempt of partial combining these two approaches is done in the present work: the pressure and temperature fields in the reservoir are determined by solving the problem of non-

[1] **Proceedings of the 14th international workshop on computer science and information technologies CSIT'2012, Ufa – Hamburg – Norwegian Fjords, 2012**

isothermal filtration of an imperfect gas and are compared with equilibrium conditions of hydrate formation. This solution can be further used to determine the temperature and pressure in the bottom hole region.

2. Formulation of the problem

For the mathematical description of gas production from a single well located at the center of a circular gas reservoir, we use a system of equations that describe non-isothermal filtration of an imperfect gas in a porous medium where the energy transfer due to heat conduction is assumed to be negligible as compared to convective transfer [3]:

$$\frac{\partial}{\partial \bar{t}}\left(\frac{\bar{p}}{Z\bar{T}}\right)=\frac{1}{\bar{r}}\frac{\partial}{\partial \bar{r}}\left(\bar{r}\frac{\bar{p}}{Z\bar{T}}\frac{\partial \bar{p}}{\partial \bar{r}}\right),\ \bar{r}_{\mathrm{w}}<\bar{r}<\bar{r}_{\mathrm{k}},\ \bar{t}>0. \quad (1)$$

$$\frac{\partial \bar{T}}{\partial \bar{t}}=\left(1+\frac{\bar{T}}{Z}\frac{\partial Z}{\partial \bar{T}}\right)\frac{\partial \bar{p}}{\partial \bar{t}}+\frac{c_{\mathrm{p}}}{R}\frac{\bar{p}}{Z\bar{T}}\frac{\partial \bar{T}}{\partial \bar{r}}\frac{\partial \bar{p}}{\partial \bar{r}}- -\frac{\bar{T}}{Z}\frac{\partial Z}{\partial \bar{T}}\left(\frac{\partial \bar{p}}{\partial \bar{r}}\right)^2,\ \bar{r}_{\mathrm{w}}<\bar{r}<\bar{r}_{\mathrm{k}},\ \bar{t}>0, \quad (2)$$

where

$$\bar{p}=\frac{p}{p_0},\ \bar{r}=\frac{r}{l},\ \bar{r}_{\mathrm{w}}=\frac{r_{\mathrm{w}}}{l},\ \bar{r}_{\mathrm{k}}=\frac{r_{\mathrm{k}}}{l},$$

$$\bar{t}=\frac{\kappa_{\mathrm{p}}t}{l^2},\ \bar{T}=\frac{c_{\mathrm{r}}T}{mp_0},\ \kappa_{\mathrm{p}}=\frac{kp_0}{m\mu}.$$

In what follows, the bar above the dimensionless variables is omitted for convenience.

The pressure on the well face is assumed to be constant:

$$p=p_{\mathrm{w}},\ r=r_{\mathrm{w}}. \quad (3)$$

Conditions modeling the absence of the filtered gas and heat fluxes are imposed on the external boundary, i.e., the water-driven regime of gas production is modeled:

$$\frac{\partial p}{\partial r}=0,\ \frac{\partial T}{\partial r}=0,\ r=r_{\mathrm{k}}. \quad (4)$$

At the initial time, the pressure and temperature are assumed to be constant:

$$p(r,0)=1,\ T(r,0)=T_0,\ r_{\mathrm{w}}\le r\le r_{\mathrm{k}}. \quad (5)$$

The equation of state is the Latonov – Gurevich equation [3]:

$$Z=\left(0.17376\ln\left(\frac{mp_0}{c_{\mathrm{r}}T_{\mathrm{c}}}T\right)+0.73\right)^{\frac{p_0}{p_{\mathrm{c}}}p}+0.1\frac{p_0}{p_{\mathrm{c}}}p, \quad (6)$$

where T_{c} and p_{c} are the critical values of temperature and pressure of the natural gas, which is a mixture of gases, mainly of the paraffin series, beginning from methane.

Thus, the solution of the initial-boundary problem (1)–(6) depends on the parameter c_{p}/R included into (2), on the boundary condition (3) determined by the dimensionless pressure p_{w}, and on two dimensionless complexes $mp_0/c_{\mathrm{r}}T_{\mathrm{c}}$ and p_0/p_{c} involved into (6). It should be noted that the gas temperature at the bottom hole (at $r=r_{\mathrm{w}}$) in the problem formulation used is a sought quantity determined in the course of solving the problem, and (2) is a quasi-linear hyperbolic equation of the first order. The characteristics of this equation start from the right boundary; therefore, the boundary condition of the absence of the heat flux (4) is sufficient for determining the unique solution of this equation. In addition to calculating the temperature and pressure fields, we determined the total amount of the extracted gas $V=\int_0^t A(t)dt$, where $A=\left.\frac{p}{ZT}\frac{\partial p}{\partial r}\right|_{r=r_{\mathrm{w}}}$ is the dimensionless mass flow rate expressed via the dimensional quantities as $A=\frac{m\mu RM}{2\pi kH p_0 c_{\mathrm{r}}}$.

3. Numerical implementation of the model and its algorithm

For solving the initial-boundary problem (1)–(6), replacing $p(r_i,t_j)=p_i^j$ and $T(r_i,t_j)=T_i^j$ by numerical analogs in grid nodes, (1) is approximated by a purely implicit, absolutely stable difference scheme similar to the scheme that was derived for a plane-parallel problem in [5]:

$$\left(\frac{{}^{s+1}p_i^{j+1}}{{}^{s}Z_i^{j+1}\,{}^{s}T_i^{j+1}}-\frac{{}^{s}p_i^{j}}{{}^{s}Z_i^{j}\,{}^{s}T_i^{j}}\right)\frac{r_i}{\tau}={}^{s}k_{i+1}\left(\frac{{}^{s+1}p_{i+1}^{j+1}-{}^{s+1}p_i^{j+1}}{h^2}\right)- -{}^{s}k_i\left(\frac{{}^{s+1}p_i^{j+1}-{}^{s+1}p_{i-1}^{j+1}}{h^2}\right),\ i=\overline{1,n-1},\ j=\overline{0,j_0-1}. \quad (7)$$

The difference approximation of the boundary condition (3) has the form

$${}^{s+1}p_0^{j+1}=p_{\mathrm{w}},\ j=\overline{0,j_0-1}. \quad (8)$$

The difference analog of the first boundary condition (4) is written with the second order of approximation. To obtain the difference scheme for the external boundary ($i=n$), we integrate (1) in the elementary cell $[r_n-h/2,r_n]$ and find

$$\left(\frac{{}^{s+1}p_n^{j+1}}{{}^{s}Z_n^{j+1}\,{}^{s}T_n^{j+1}}-\frac{{}^{s}p_n^{j}}{{}^{s}Z_n^{j}\,{}^{s}T_n^{j}}\right)\frac{hr_n}{2\tau}=-{}^{s}k_n\frac{{}^{s+1}p_n^{j+1}-{}^{s+1}p_{n-1}^{j+1}}{h},\quad(9)$$

$$j=\overline{0,\,j_0-1}.$$

As the function $T(r,t)$ is sufficiently smooth, then it is reasonable to put (2) into correspondence to an unconditionally stable implicit difference scheme of the "corner" type [6]:

$$\frac{{}^{s+1}T_i^{j+1}-{}^{s}T_i^{j}}{\tau}=\left(1+{}^{s}a_i\,{}^{s+1}T_i^{j+1}\right)\left(\frac{{}^{s+1}p_i^{j+1}-{}^{s}p_i^{j}}{\tau}\right)-$$

$$-{}^{s}d_i\,{}^{s+1}T_i^{j+1}+{}^{s}b_i\left(\frac{{}^{s+1}T_{i+1}^{j+1}-{}^{s+1}T_i^{j+1}}{h}\right),\quad(10)$$

$$i=\overline{0,n-1},\ j=\overline{0,\,j_0-1}.$$

Taking into account condition (4) for the external boundary ($i=n$), we obtain the scheme

$$\frac{{}^{s+1}T_n^{j+1}-{}^{s}T_n^{j}}{\tau}=\left(1+{}^{s}a_n\,{}^{s+1}T_n^{j+1}\right)\left(\frac{{}^{s+1}p_n^{j+1}-{}^{s}p_n^{j}}{\tau}\right)-\quad(11)$$

$$-{}^{s}d_n\,{}^{s+1}T_n^{j+1},\quad j=\overline{0,\,j_0-1}.$$

This approximation is justified because, as it follows from the second term in the right side of (2), the slope of the characteristics does not change its sign since the sign of the derivative of pressure with respect to the spatial coordinate is unchanged (the remaining terms are always positive). Therefore, the quantities involved into the difference (10) and (11), in particular, those included into the coefficient ${}^{s}b_i$, do not change their sign either. The initial conditions are approximated in the form

$${}^{s}p_i^{0}=1,\quad {}^{s}T_i^{0}=T_0,\quad i=\overline{0,n}.\quad(12)$$

The following notation is used in (7)–(11):

$${}^{s}k_i=\frac{{}^{s}r_{i-1/2}\,{}^{s}p_{i-1/2}^{j+1}}{{}^{s}Z_{i-1/2}^{j+1}\,{}^{s}T_{i-1/2}^{j+1}},\quad r_{i-1/2}=\frac{r_{i-1}+r_i}{2},$$

$${}^{s}p_{i-1/2}^{j+1}=\frac{{}^{s}p_{i-1}^{j+1}+{}^{s}p_i^{j+1}}{2},\quad {}^{s}T_{i-1/2}^{j+1}=\frac{{}^{s}T_{i-1}^{j+1}+{}^{s}T_i^{j+1}}{2},$$

$${}^{s}a_i=\frac{1}{{}^{s}Z_i^{j+1}}\left(\frac{{}^{s}\partial Z}{\partial T}\right)_i^{j+1},\quad {}^{s}a_n=\frac{1}{{}^{s}Z_n^{j+1}}\left(\frac{{}^{s}\partial Z}{\partial T}\right)_n^{j+1},$$

$${}^{s}b_i=\frac{c_p}{R}\frac{{}^{s+1}p_i^{j+1}}{{}^{s}Z_i^{j+1}\,{}^{s}T_i^{j+1}}\frac{{}^{s+1}p_{i+1}^{j+1}-{}^{s+1}p_{i-1}^{j+1}}{2h},$$

$${}^{s}d_i={}^{s}a_i\left(\frac{{}^{s+1}p_{i+1}^{j+1}-{}^{s+1}p_{i-1}^{j+1}}{2h}\right)^2,\quad {}^{s}d_n={}^{s}a_n\left(\frac{{}^{s+1}p_n^{j+1}-{}^{s+1}p_{n-1}^{j+1}}{h}\right)^2.$$

For numerical implementation of the difference problem (7)–(12), we use the method of simple iterations at each time layer. The iterative process is organized as follows:

a) set $s=0$, ${}^{0}p_i^{j+1}=p_i^{j}$, ${}^{0}T_i^{j+1}=T_i^{j}$, $i=\overline{0,n}$;

b) using the sweep method, solve a linearized system of three-point algebraic equations with respect to unknown values of pressure at the nodes of the spatial grid ${}^{s+1}p_i^{j+1}$, $i=\overline{0,n}$:

$${}^{s+1}p_0^{j+1}=p_w;$$

$$A_i\,{}^{s+1}p_{i-1}^{j+1}-C_i\,{}^{s+1}p_i^{j+1}+B_i\,{}^{s+1}p_{i+1}^{j+1}=-F_i,\quad i=\overline{1,n-1};$$

$$A_n\,{}^{s+1}p_{n-1}^{j+1}-C_n\,{}^{s+1}p_n^{j+1}=-F_n;$$

where

$$A_i=\frac{{}^{s}k_i}{h^2},\quad C_i=\frac{{}^{s}k_i}{h^2}+\frac{{}^{s}k_{i+1}}{h^2}+\frac{r_i}{\tau\,{}^{s}Z_i^{j+1}\,{}^{s}T_i^{j+1}},\quad B_i=\frac{{}^{s}k_{i+1}}{h^2},$$

$$F_i=\frac{{}^{s}r_i\,{}^{s}p_i^{j}}{\tau\,{}^{s}Z_i^{j}\,{}^{s}T_i^{j}},\quad A_n=\frac{{}^{s}k_n}{h},\quad C_n=\frac{{}^{s}k_n}{h}+\frac{h\,r_n}{2\tau\,{}^{s}Z_n^{j+1}\,{}^{s}T_n^{j+1}},$$

$$F_n=\frac{hr_n}{2\tau}\frac{{}^{s}p_n^{j}}{{}^{s}Z_n^{j}\,{}^{s}T_n^{j}};$$

c) with the pressure values found, determine the temperature distribution by the recurrent formulas

$$
{}^{s+1}T_n^{j+1} = \frac{\dfrac{{}^{s+1}T_n^{j}}{\tau} + \left(\dfrac{{}^{s+1}p_n^{j+1} - {}^{s+1}p_n^{j}}{\tau} \right)}{\dfrac{1}{\tau} - {}^{s}a_n \left(\dfrac{{}^{s+1}p_n^{j+1} - {}^{s+1}p_n^{j}}{\tau} \right) + {}^{s}d_n};
$$

$$
{}^{s+1}T_i^{j+1} = \frac{\dfrac{{}^{s+1}T_i^{j}}{\tau} + \left(\dfrac{{}^{s+1}p_i^{j+1} - {}^{s+1}p_i^{j}}{\tau} \right) + {}^{s}b_i \dfrac{{}^{s+1}T_{i+1}^{j+1}}{h}}{\dfrac{1}{\tau} - {}^{s}a_i \left(\dfrac{{}^{s+1}p_i^{j+1} - {}^{s+1}p_i^{j}}{\tau} \right) + \dfrac{{}^{s}b_i}{h} + {}^{s}d_i}, \quad i = \overline{n-1, 0};
$$

d) check whether the conditions of convergence of iterations are satisfied:

$$
\max_{i=0,n} \left| {}^{s+1}p_i^{j+1} - {}^{s}p_i^{j+1} \right| < \varepsilon_1, \quad \max_{i=0,n} \left| {}^{s+1}T_i^{j+1} - {}^{s}T_i^{j+1} \right| < \varepsilon_2.
$$

If these conditions are not satisfied, increase s by unity and return to item (b); if they are satisfied, go to the next time layer.

4. Results and discussion

In our computational experiment, we studied the influence of the pressure at the well bottom hole p_w on the dynamics of temperature and pressure variations in the reservoir. In addition, we estimated the effect of the frequently used assumption on isothermality of the filtration process on the pressure field and on the total gas production. The calculations were performed for two typical gas fields of Northern Russia: the Sredne-Vilyuiskoe in the Sakha Republic (Yakutiya) and the well known Messoyakha gas field which differs from the first one by more shallow gas reservoir depth and, therefore, much lower pressure and temperature. For the first gas field the parameters of calculations were as follows: $p_w = 14$ MPa and $p_w = 22$ MPa; the parameters $c_p/R = 5.118$ and $c_r/mp_0 = 1.234$, the initial temperature of the reservoir $T_0 = 323$ K, and the initial pressure $p_0 = 24$ MPa had constant values. The critical parameters $T_c = 205.022$ K and $p_c = 4.6596$ MPa were determined by the method described in [7]. The equilibrium temperature of hydrate formation was calculated by the formula $T_{ph}(p) = a \ln p + b$, where the constants $a = 7.01$ K and $b = 178.28$ K were found by means of approximating the thermodynamic equilibrium curve determined by Sloan's method [8] for a known composition of the gas (vol. %): $CH_4 - 90.34$, $C_2H_6 - 4.98$, $C_3H_8 - 1.74$, $iC_4H_{10} - 0.22$, $nC_4H_{10} - 0.41$, $C_5H_{12+} - 1.55$, $CO_2 - 0.28$, $N_2 - 0.48$.

The calculations show that the changes in the temperature field are significant only in the case of an intense depression on the gas-bearing reservoir, when $p_w = 14$ MPa. Even in this case, however, they are localized in a narrow zone near the well, which is clearly seen in fig. 1. At small values of the dimensionless time t, this zone does not exceed 4 m (curve 1), while the temperature in the remaining part of the reservoir is equal to its initial value. At the end of the computational process, there is a drastic decrease in temperature at a distance of 8 m from the bottom hole; the temperature at greater distances is almost constant and lower than the initial value (curve 2).

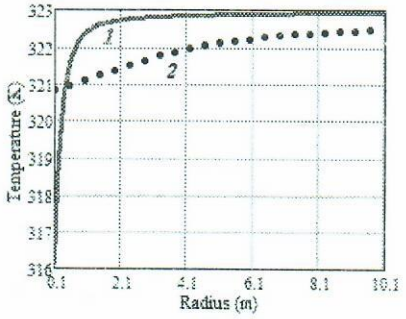

Fig. 1. Temperature distribution at $p_w = 14$ MPa; $t = 200$ (curve 1) and $t = 1600000$ (curve 2)

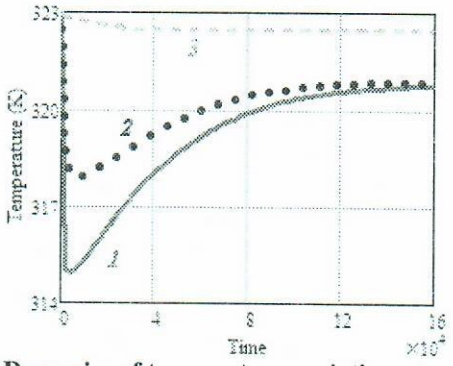

Fig. 2. Dynamics of temperature variation at $p_w = 14$ MPa; $r = 0.1$ m (curve 1), $r = 0.3$ m (curve 2), and $r = 10.1$ m (curve 3)

A more detailed analysis shows that the temperature at the bottom hole drastically decreases at first (in the example considered, this decrease reached 8 K), and then starts to recover (curve 1 in fig. 2). The same trend is also observed at a small distance from the bottom hole, but the decrease in the temperature was 5 K (curve 2 in fig. 2). Already at a distance of 10 m, however, there is only a minor decrease in temperature with time (curve 3 in fig. 2).

Let us now estimate the influence of the input parameters and the temperature field on the dynamics of variation of

the pressure field. It is obvious from physical considerations that the pressure value at the point of gas extraction should be an important parameter determining the spatial variations of pressure in time.

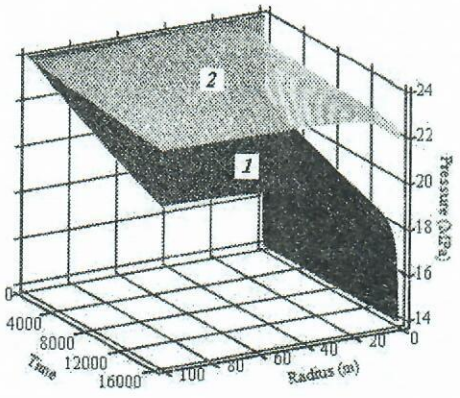

Fig. 3. Dynamics of the pressure field; $p_w = 14$ MPa (surface 1) and $p_w = 22$ MPa (surface 2)

This is clearly seen in fig. 3, which shows a comparison of two variants of the bottom hole pressure behavior, other conditions being identical: in the first variant, the pressure changes significantly at all points of the reservoir; in the second variant, these changes occur only in a narrow zone near the well even at large values of the dimensionless time t. For a detailed analysis of the role of the temperature field in the dynamics of the pressure distribution, we analyze the curves in figs. 4 and 5. It is seen that the effect of the temperature field is small; in the case of intense gas extraction, i.e., at $p_w = 14$ MPa, the pressure decrease is underestimated by 0.1 MPa only (cf. curves 1, 2 and 3, 4 in fig. 4 and curves 1, 2 in fig. 5a). A similar situation is observed in the case of gas extraction with much lower intensity, but here the pressure decrease is overestimated (cf. curves 1, 2 in fig. 5a with similar curves in fig. 5b).

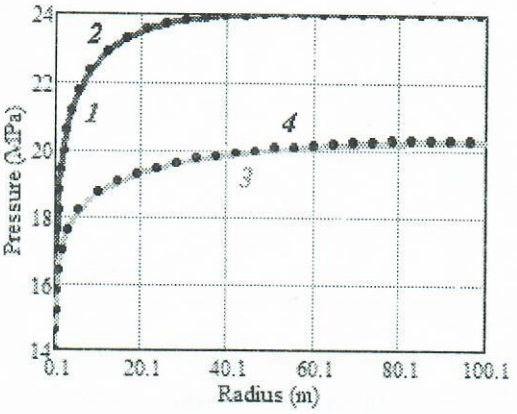

Fig. 4. Pressure distributions at $p_w = 14$ MPa; the solid and dotted curves refer to non-isothermal and isothermal regimes, respectively; $t = 200$ (curves 1 and 2) and $t = 20000$ (curves 3 and 4)

It is important to note that the above-indicated features of non-isothermality manifestation are also observed at the intermediate stage of the process ($t = 160000$): the difference is not great in the case of high intensity of gas extraction (curves 1, 2 in fig. 6a), but the underestimation of the pressure decrease in the case with low intensity of gas extraction reaches almost 0.2 MPa, which is clearly seen in fig. 6b. It should also be noted that the pressure rapidly reaches a steady regime in the case with low intensity of gas extraction, and this state in the isothermal model is reached earlier than in the non-isothermal model (cf. curves 1 and 2 in fig. 6b).

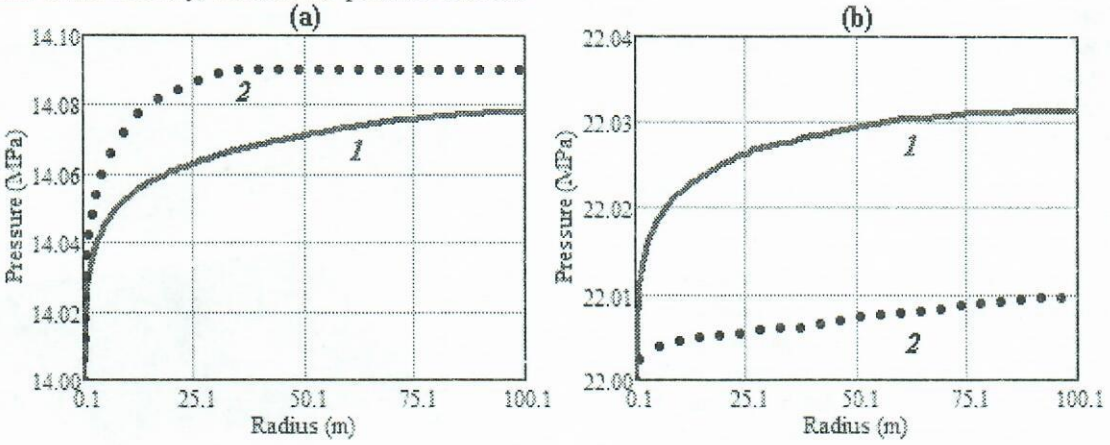

Fig. 5. Pressure at the end of the calculated time; curves 1 and 2 refer to non-isothermal and isothermal regimes, respectively; $p_w = 14$ MPa (a) and $p_w = 22$ MPa

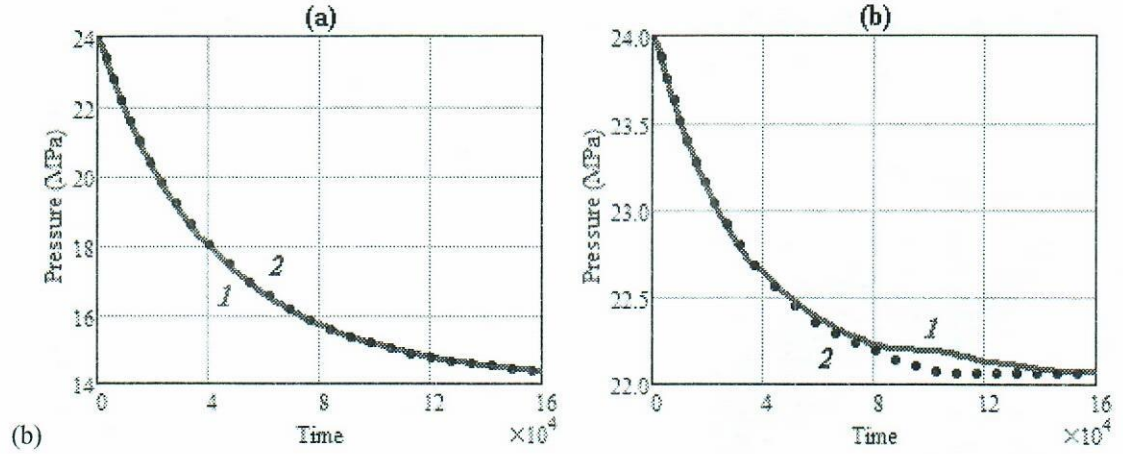

Fig. 6. Pressure at the reservoir boundary; curves 1 and 2 refer to the non-isothermal and isothermal regimes, respectively; $p_w = 14$ MPa (a) and $p_w = 22$ MPa (b)

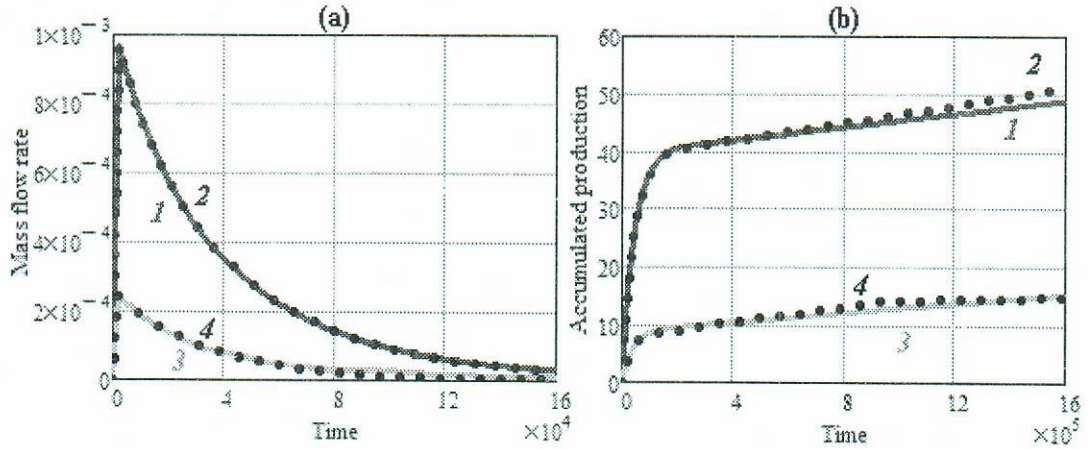

Fig. 7. Mass production of the gas (a) and accumulated gas production (b); the solid and dotted curves refer to non-isothermal and isothermal regimes, respectively; $p_w = 14$ MPa (curves 1 and 2) and $p_w = 22$ MPa (curves 3 and 4)

The non-isothermality insignificantly effects predicting of the total gas production (fig. 7). Let us also note that all curves in fig. 7b have two typical, almost rectilinear segments, with the inflection corresponding to the transition to the deposit depletion regime.

Let us estimate the possibility of hydrate formation at the bottom hole of the well. For this purpose, we compare the temperature field in this zone with the equilibrium conditions of hydrate formation. The results of this comparison are shown in fig. 8. It is seen that even in the case of intense gas extraction the gas temperature is always above the equilibrium temperature of hydrate formation. This result is completely proven by the multiyear history of gas production from the field.

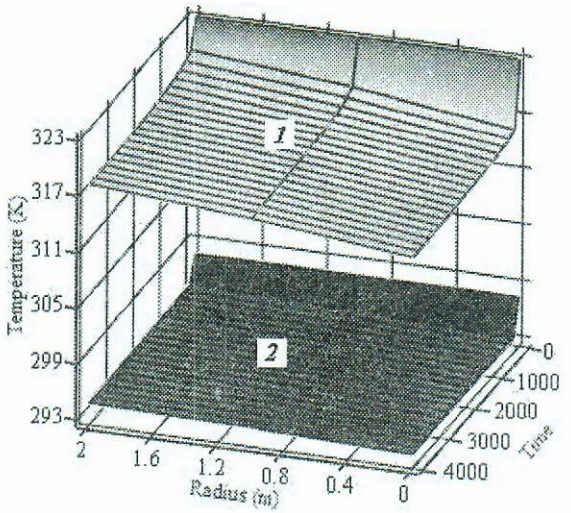

Fig. 8. Temperature at the bottom hole at $p_w = 14$ MPa; gas temperature (surface 1) and equilibrium temperature of hydrate formation (surface 2)

Consider now the results of analogous calculations for the Messoyakha gas field. The initial data: $c_p/R = 5.278$, $c_r/mp_0 = 3.415$ 1/K, $T_0 = 282.91$ K, $p_0 = 6.8$ MPa, $T_c = 191.202$ K, $p_c = 4.6893$ MPa, $a = 10.036$ K, $b = 126.023$ K, $p_w = 5.3$ MPa and $p_w = 6.3$ MPa; composition of the gas (vol. %): $CH_4 - 99.169$, $C_2H_6 - 0.003$, $C_3H_8 - 0.009$, $iC_4H_{10} - 0.002$, $nC_4H_{10} - 0.002$, $C_5H_{12+} - 0.018$, $CO_2 - 0.611$, $N_2 - 0.186$.

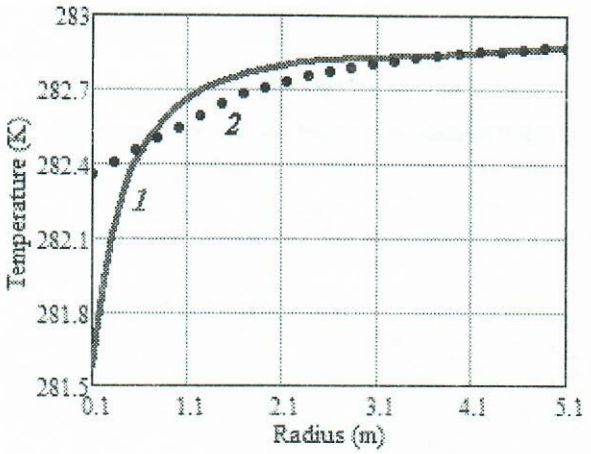

Fig. 9. Temperature distribution at $p_w = 5.3$ MPa; $t = 5000$ (curve 1) and $t = 1600000$ (curve 2)

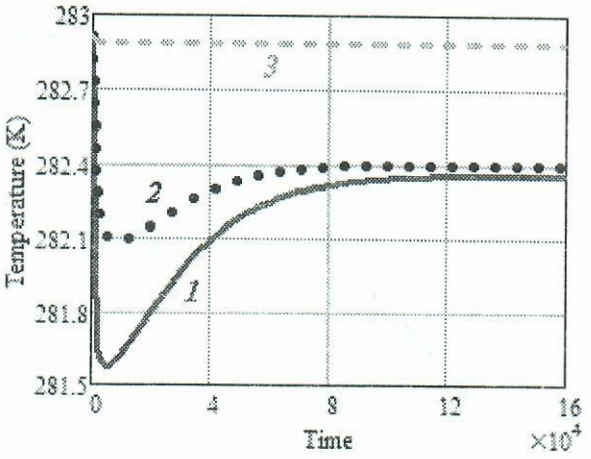

Fig. 10. Dynamics of temperature variation at $p_w = 5.3$ MPa; $r = 0.1$ m (curve 1), $r = 0.3$ m (curve 2), and $r = 10.1$ m (curve 3)

The basic results of the computational experiment are very close to the previous example: the changes of the temperature are localized in a narrow zone near the well (fig. 9 and 10); in the case of intense gas extraction the pressure changes significantly through the entire reservoir; in the case with low intensity of gas extraction these changes occur only in a narrow zone near the well (fig. 11).

The influence of the temperature field on the pressure redistribution in the reservoir (figs. 12–14) is also insignificant. In spite of this fact it may lead to substantial underestimation of total gas extraction: about 20% for high-intensity (curves *1* and *2*) and 34% for low-intensity gas production (curves *3* and *4*). It means that isothermal filtration model will leads to underestimation of gas field potential

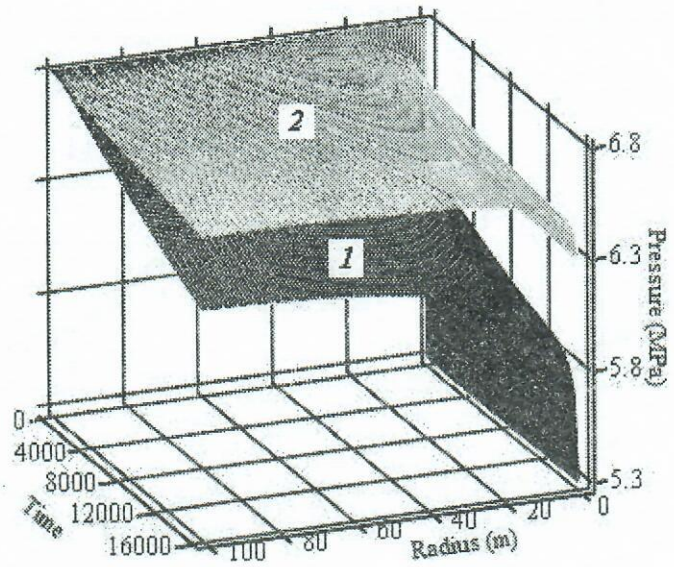

Fig. 11. Dynamics of the pressure field; $p_w = 5.3$ MPa (surface 1) and $p_w = 6.3$ MPa (surface 2)

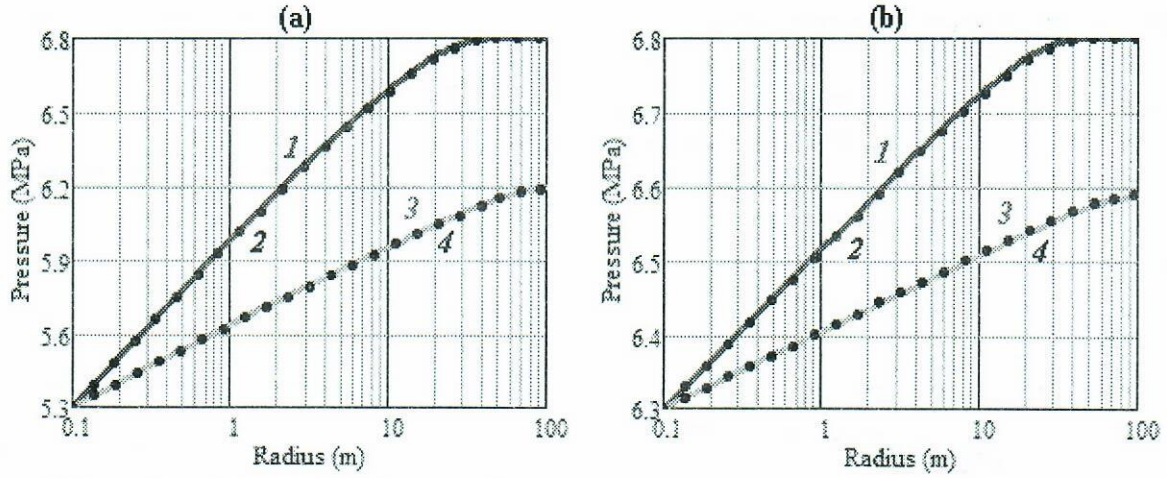

Fig. 12. Pressure distributions; the solid and dotted curves refer to non-isothermal and isothermal models, respectively; $t = 200$ (curves 1 and 2) and $t = 20000$ (curves 3 and 4); $p_w = 5.3$ MPa (a) and $p_w = 6.3$ MPa (b)

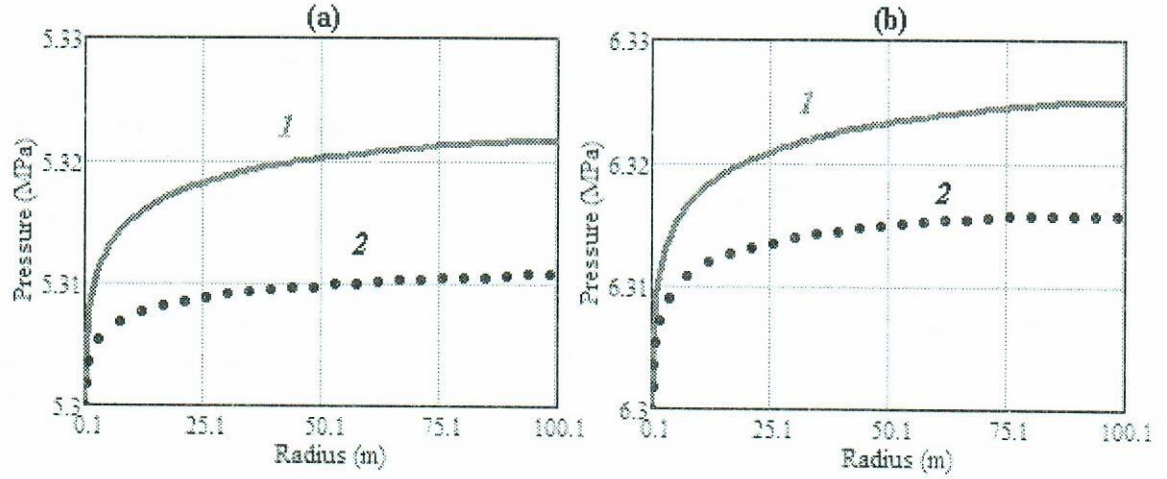

Fig. 13. Pressure at the end of the calculated time; curves 1 and 2 refer to non-isothermal and isothermal models, respectively; $p_w = 5.3$ MPa (a) and $p_w = 6.3$ MPa (b)

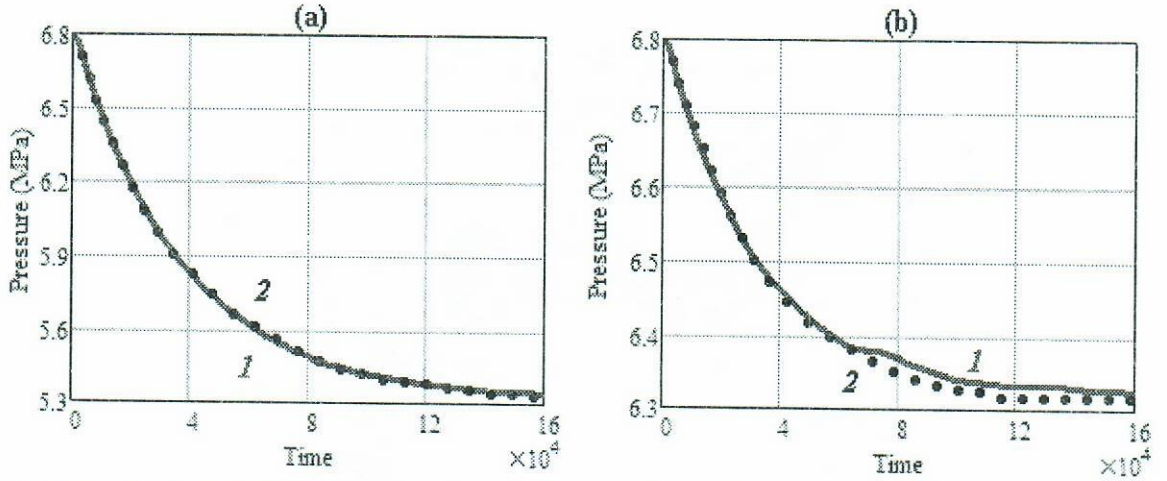

Fig. 14. Pressure at the reservoir boundary; curves 1 and 2 refer to the non-isothermal and isothermal models, respectively; $p_w = 5.3$ MPa (a) and $p_w = 6.3$ MPa (b)

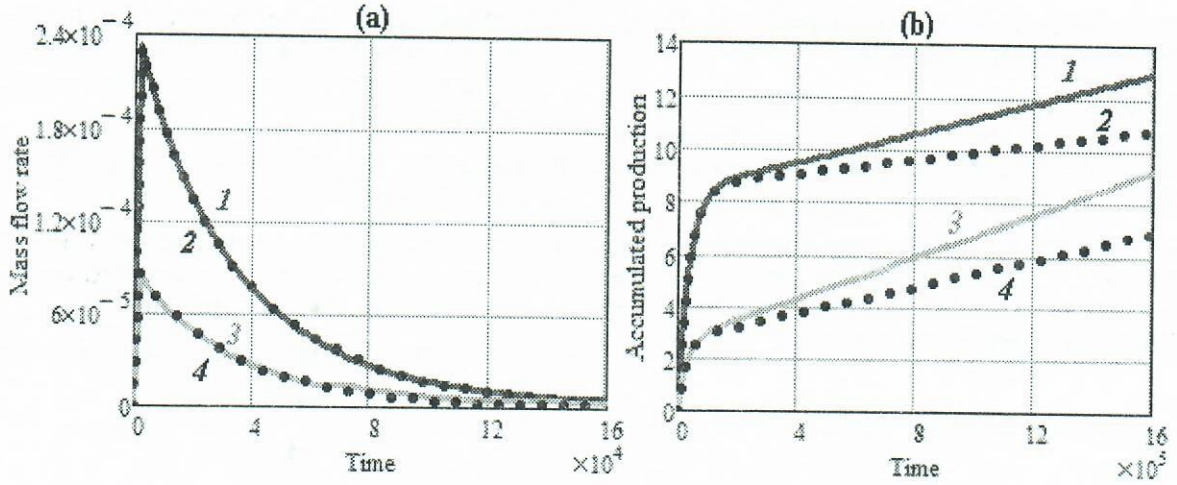

Fig. 15. Mass flow rate of the gas (a) and cumulative gas production (b); the solid and dotted curves refer to nonisothermal and isothermal models, respectively; $p_w = 5.3$ MPa (curves 1 and 2) and $p_w = 6.3$ MPa (curves 3 and 4)

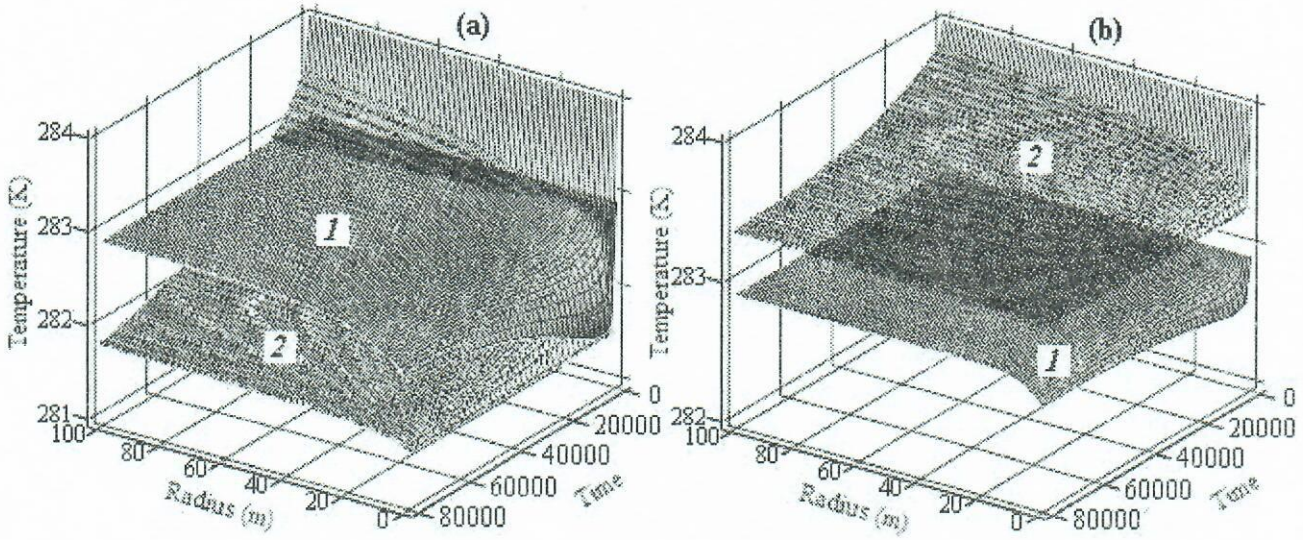

Fig. 16. Temperature at the bottom hole region; gas temperature (surface 1) and equilibrium temperature of hydrate formation (surface 2); $p_w = 5.3$ MPa (a) and $p_w = 6.3$ MPa (b)

Finally, we will estimate the possibility of hydrate formation at the bottom hole of the well. The results are shown in fig. 16. It is seen that in the case of intense gas production its temperature is above the equilibrium temperature of hydrate formation everywhere except a narrow zone near the well but only at the initial period of production (fig. 16a). But if the depression is smaller, gas temperature will always be lower than hydrate equilibrium temperature (fig. 16b). Such unexpected result has a clear explanation. At the conditions given the decrease of hydrate equilibrium temperature due to pressure decrease is more significant than common gas cooling due to Joule – Thomson effect and heat exchange with surrounding rocks. Certainly, these results are valid only for the initial data indicated above. Nevertheless, it allows two important conclusions to be drawn: 1) such a zone can be identified with the use of some geophysical method, for instance, acoustic logging; 2) such a narrow zone can be easily affected by one of hydrate formation inhibitors (methanol or calcium chloride solution).

These results again demonstrate the importance of taking into account thermodynamic processes in mathematical modeling of natural gas production.

5. References

1. Bondarev E.A., Gabysheva L.N. and Kanibolotskii M.A. "Modeling of Hydrate Formation during Gas Motion in Tubes". *Izv. Akad. Nauk SSSR, Mekh. Zhidk. Gaza*. 1982; 5: 105-112.
2. Bondarev E.A. and Argunova K.K. "Mathematical models of hydrate formation in gas wells". In: *Information and Mathematical Technologies in Science and Management, Proc. XIV Baikal All-Russian Conf. on Information and Mathematical*

Technologies in Science and Management. Part 3. Irkutsk, Russia, 2009, pp. 41-51.

3. Bondarev E.A., Vasil'ev V.I., Voevodin A.F., Pavlov N. N., Shadrina A.P. "Thermodynamics of Gas Production and Transportation Systems". Nauka, Novosibirsk, 1988.
4. Khairullin M.Kh., Shamsiev M.N., Morozov P.E. and Tulupov L.A. "Modeling of Hydrate Formation in the Borehole of a Vertical Gas Well". *Vychislitelnye. Tekhnologii.* 2008; vol. 13, 5: 88-94.
5. Bondarev E.A., Argunova K.K. and Rozhin I.I. "Plane-Parallel Nonisothermal Filtration of Gas: Role of Heat Transfer". *Inzh.-Fiz. Zh.* 2009; vol. 82, 6: 1059-1065.
6. Turchak L.I. "Fundamentals of Numerical Methods". Nauka, Moscow, 1987.
7. Kay W.B. "Density of Hydrocarbon Gases and Vapors at High Temperature and Pressures". *Ind. Eng. Chem. Res.* 1936; 28: 1014-1019.
8. Sloan E.D. "Clathrate Hydrates of Natural Gases". Marcel Dekker, New York, 1998.